Constitutive recycling of the store-operated Ca^{2+} channel Orai1 and its internalization during meiosis

Fang Yu, Lu Sun, and Khaled Machaca

Department of Physiology and Biophysics, Weill Cornell Medical College in Qatar, Education City, Qatar Foundation, Doha 24144, Qatar

The egg's competency to activate at fertilization and transition to embryogenesis is dependent on its ability to generate a fertilization-specific Ca^{2+} transient. To endow the egg with this capacity, Ca^{2+} signals remodel during oocyte maturation, including inactivation of the primary Ca^{2+} influx pathway store-operated Ca^{2+} entry (SOCE). SOCE inactivation is coupled to internalization of the SOCE channel, Orai1. In this study, we show that Orai1 internalizes during meiosis through a caveolin (Cav)- and dynamin-dependent endocytic pathway. Cav binds to Orai1, and we map a Cav consensus–binding site in the Orai1 N terminus, which is required for Orai1 internalization. Furthermore, at rest, Orai1 actively recycles between an endosomal compartment and the cell membrane through a Rho-dependent endocytic pathway. A significant percentage of total Orai1 is intracellular at steady state. Store depletion completely shifts endosomal Orai1 to the cell membrane. These results define vesicular trafficking mechanisms in the oocyte that control Orai1 subcellular localization at steady state, during meiosis, and after store depletion.

Introduction

Vertebrate oocytes are arrested in prophase of meiosis I in an interphase-like stage of the cell cycle with an intact germinal vesicle (nucleus; Masui and Clarke, 1979). Before such oocytes become fertilization competent, they undergo a cellular differentiation pathway known as oocyte maturation, during which they complete meiosis I and arrest at metaphase of meiosis II. We refer to these mature oocytes as eggs. Oocyte maturation encompasses remodeling of Ca^{2+} signaling pathways to endow the egg with the capacity to activate at fertilization and undergo the egg to embryo transition (Machaca, 2007). The fertilization-specific Ca^{2+} signal provides a digital cipher that encodes critical cellular events at fertilization in a sequential fashion, including the block to polyspermy and completion of meiosis. As part of Ca^{2+} signaling remodeling, the primary Ca^{2+} influx pathway, store-operated Ca^{2+} entry (SOCE), inactivates (Machaca and Haun, 2000; Machaca and Haun, 2002). SOCE inhibition could contribute to shaping the dynamics of the fertilization-specific Ca^{2+} transient and may represent a safety mechanism to prevent premature egg activation (Machaca and Haun, 2002; Ullah et al., 2007). SOCE also inactivates during mitosis of mammalian cells (Preston et al., 1991; Tani et al., 2007).

SOCE is activated by the level of Ca^{2+} in intracellular stores, primarily the ER. Lowering free ER Ca^{2+} below a certain threshold activates Ca^{2+} influx at the cell membrane through SOCE. RNAi screens identified the critical molecular determinants of SOCE. The stromal interaction molecule 1 (STIM1), an ER transmembrane protein with luminal EF-hands, was identified as the ER Ca^{2+} sensor (Liou et al., 2005; Roos et al., 2005), and Orai1 (also known as CRACM1) as the Ca^{2+} release-activated current channel (Feske et al., 2006; Vig et al., 2006; Zhang et al., 2006). The Orai1 protein spans the membrane four times with intracellular N and C termini, has no sequence homology to other known channels, and is essential for Ca^{2+} release-activated current (Prakriya et al., 2006; Vig et al., 2006; Yeromin et al., 2006). A mutation in *Orai1* (R91W) abrogates Ca^{2+} influx in T cells and causes severe combined immunodeficiency disorder (Feske et al., 2006). Depletion of Ca^{2+} stores releases Ca^{2+} from the STIM1 luminal EF-hand, resulting in a conformational change that leads to clustering of STIM1 into large puncta in a cortical ER domain that localizes 10–20 nm below the cell membrane (Wu et al., 2006; Liou et al., 2007; Stathopulos et al., 2008; Orci et al., 2009). Clustered STIM1

F. Yu and L. Sun contributed equally to this paper.

Correspondence to Khaled Machaca: Khm2002@qatar-med.cornell.edu

Abbreviations used in this paper: Cav, caveolin; CTB, cholera toxin B; GVBD, germinal vesicle breakdown; MβCD, methyl–β-cyclodextrin; SOCE, store-operated Ca^{2+} entry; STIM1, stromal interaction molecule 1.

The Rockefeller University Press $30.00
J. Cell Biol. Vol. 191 No. 3 523–535
www.jcb.org/cgi/doi/10.1083/jcb.201006022

recruits Orai1 into coincident puncta and gates the channel leading to SOCE (Luik et al., 2006; Park et al., 2009; Yuan et al., 2009). STIM1 has also been shown to couple to and gate transient receptor potential canonical channels to induce SOCE (Huang et al., 2006; Yuan et al., 2007).

As with other ion channels, SOCE current amplitude depends in part on the levels of the channel protein in the target membrane. Indeed, defects in ion channel trafficking lead to serious clinical consequences. For example, a mutation in CFTR (ΔF508) produces a functional Cl^- channel that never reaches the plasma membrane, thus hampering Cl^- transport and leading to cystic fibrosis (Skach, 2000). Defects in ether-a-go-go (hERG) channel trafficking lead to long QT syndrome, a cardiac disorder that increases arrhythmias and the risk of sudden cardiac death (Perrin et al., 2008). Members of the transient receptor potential canonical channel family are also regulated by vesicular insertion into the cell membrane after agonist stimulation (Bezzerides et al., 2004; Singh et al., 2004). In addition, TRPC1 function depends on its localization to lipid raft domains (Lockwich et al., 2000), and caveolin (Cav) has been implicated in TRPC1 targeting to the plasma membrane and its association with STIM1 (Brazer et al., 2003; Pani et al., 2009).

A role for vesicular trafficking in SOCE was initially proposed in the context of the coupling mechanism between store depletion and SOCE activation based on the role of GTP in the process (Fasolato et al., 1993; Somasundaram et al., 1995). It was suggested that a secretion-like mechanism mediates translocation of the SOCE channel from an intracellular vesicular pool to the cell membrane, where it mediates Ca^{2+} influx. As with other early models of the SOCE coupling mechanism, this proposal was controversial. Broad action drugs that block vesicular transport, such as brefeldin A and primaquine, produce variable effects on SOCE dependent on the study (Somasundaram et al., 1995; Gregory and Barritt, 1996; Yao et al., 1999). A potential role for vesicular transport in SOCE was also implied through the effect of interventions that altered the cortical cytoskeleton (Patterson et al., 1999; Rosado et al., 2000). More specific approaches targeted at inhibiting different components of the SNARE machinery required for vesicular fusion also produced conflicting results (Yao et al., 1999; Alderton et al., 2000; Bakowski et al., 2003; Scott et al., 2003). It is difficult to reconcile these early findings with our current knowledge of the SOCE activation mechanism centered around STIM1–Orai1 modulation and interaction. Although significant knowledge has accumulated regarding STIM1 subcellular distribution dynamics (Lewis, 2007; Fahrner et al., 2009; Lee et al., 2010), little is known about the trafficking of Orai1. We have recently shown that Orai1 is gradually internalized during *Xenopus laevis* oocyte meiosis without any associate decrease in total Orai1 protein levels, arguing that it is not targeted for degradation (Yu et al., 2009). Furthermore, Orai1 recycles at rest, and its cell membrane enrichment requires a functional exocytic machinery because Orai1 distribution shifts intracellularly in cells expressing a dominant-negative SNAP-25 that blocks exocytosis (El Jouni et al., 2007; Yu et al., 2009). Herein, we define the endocytic mechanisms controlling both Orai1 internalization during meiosis and its recycling at the cell membrane at rest. We show that Orai1 constitutively recycles between the recycling endosome and the cell membrane through a Rho- and Rab5-dependent and largely dynamin-independent endocytic pathway. During meiosis, Orai1 trafficking shifts its dependence, leading to internalization to a late endosome compartment through a Cav-, Rab5-, and dynamin-dependent endocytic pathway. Interestingly, store depletion leads to a complete shift of the subcellular distribution of Orai1 away from the endosomal compartment into the cell membrane, showing that dynamic recycling of Orai1 in the oocyte is important to regulate channel density at the cell membrane. We further map Orai1 domains required for internalization and show a dependency on both the N- and C-terminal cytoplasmic domains for targeting Orai1 for internalization. We map a Cav-binding site in the Orai1 N terminus, which is required for internalization. These results define the regulation Orai1 trafficking at rest, after store depletion, and during M phase.

Results

Expression of GFP-Orai1 with the ER marker Cherry-KDEL in oocytes shows a steady-state enrichment of Orai1 at the cell membrane, with a fraction of the protein pool localizing to an intracellular endocytic compartment (Fig. 1 A, oocyte). Orai1 distribution is shifted during meiosis, where in the egg, Orai1 is enriched in an endosomal compartment and is practically absent from the cell membrane (Fig. 1 A, egg). To confirm internalization of Orai1 during meiosis, we sought a protein that maintains its cell membrane localization during meiosis. The Ca^{2+}-activated Cl^- current is essential for the membrane depolarization observed at fertilization, which mediates the fast block to polyspermy (Machaca et al., 2001), and its amplitude is enhanced in eggs (Machaca and Haun, 2000), showing that the channel maintains its cell membrane localization. Recently, the Ca^{2+}-activated Cl^- channel was cloned from both *Xenopus* and rodents (Schroeder et al., 2008; Yang et al., 2008). We therefore synthesized the *Xenopus* TMEM16A gene and tagged it with mCherry to follow its trafficking during meiosis. TMEM16A is enriched at the cell membrane in both oocytes and eggs and, as such, is not internalized during meiosis (Fig. 1 B). Coexpression of TMEM16A with Orai1 shows colocalization of both proteins at the cell membrane in oocytes, whereas in eggs, Orai1 is enriched in endosomes and is absent from the cell membrane marked with TMEM16A (Fig. 1 B).

Identity of the Orai1-positive endosomal compartments

To identify the endocytic compartments to which Orai1 traffics in both oocytes and eggs, we expressed with GFP-Orai1 a set of tagged Rab markers that define different endocytic compartments (Fig. 1 C). Rab proteins constitute a large family of small GTPases that are central to multiple aspects of vesicular trafficking, including targeting of vesicles to the appropriate compartment and recruitment of effector proteins (Stenmark, 2009). Rab4 and Rab5 were used to visualize early endosomes, Rab11 for the recycling endosome, Rab9 and Rab7 for the late endosome (Stenmark, 2009), and LysoTracker to visualize lysosomes.

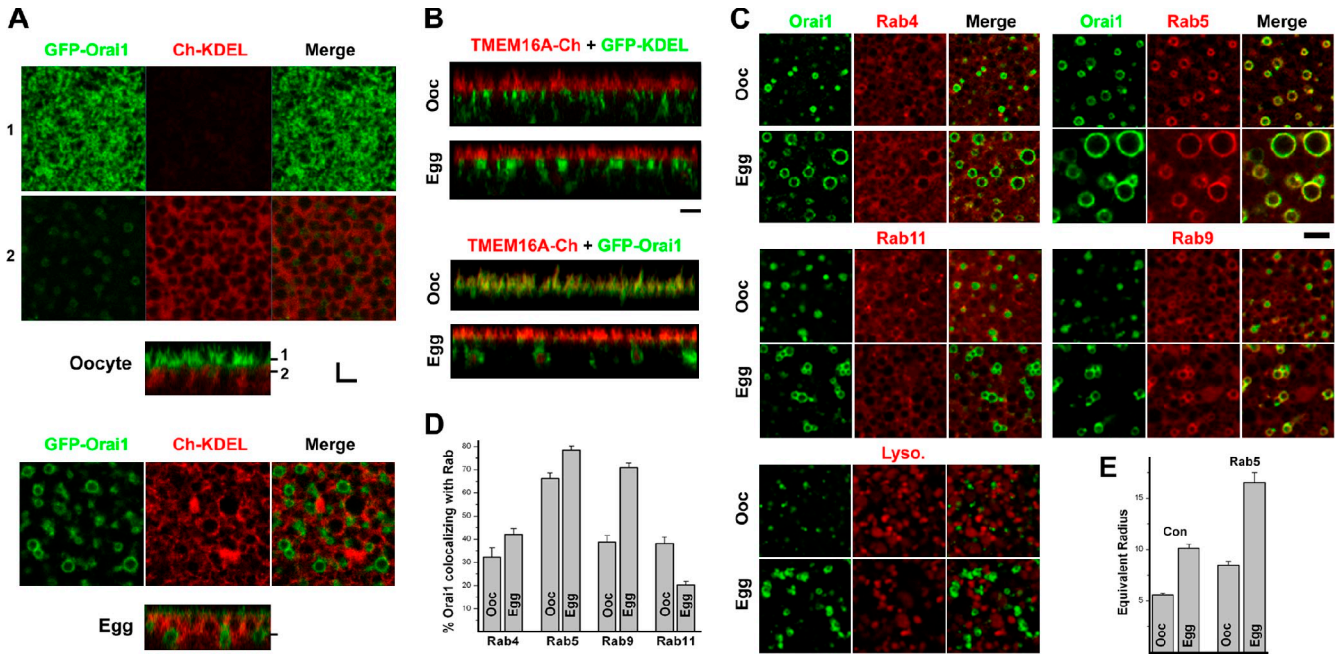

Figure 1. **Orai1 subcellular distribution at rest and during meiosis.** (A) Oocytes and eggs expressing GFP-Orai1 (2 ng RNA/cell) and the ER marker mCherry-KDEL (10 ng RNA/cell). Confocal images show two focal planes as indicated by the matching numbers (1 and 2) in the orthogonal section across the z-image stack. Bar, 3 µm. (B) Orthogonal sections from cells expressing 8 ng xTMEM16a-mCherry with either 5 ng GFP-KDEL or 2 ng GFP-Orai1. Bar, 3 µm. (C) Oocytes and eggs expressing GFP-Orai1 with endosome markers including RFP-Rab5, mCherry-tagged Rab4, Rab9, and Rab11 or stained with the lysosome marker LysoTracker. Bar, 5 µm. (D) Percentage of Orai1-positive pixels colocalizing with the Rabs (n = 10–15). (E) Equivalent endosome radius measured using MetaMorph (n = 9–13). Error bars indicate mean ± SEM.

Although most of these Rabs cycle between different endocytic compartments (Stenmark, 2009) and have a diffuse subcellular localization (Fig. 1 C), they were useful in identifying the Orai1 endocytic compartments. Rab4 exhibits diffuse distribution with some colocalization to the Orai1 endosomal compartments in oocytes and eggs (Fig. 1, C and D). Rab5 colocalizes with Orai1 in a robust and specific fashion in both oocytes and eggs (Fig. 1, C and D). Furthermore, Rab5 expression results in significantly larger Orai1-positive endosomes (Fig. 1, C and E). Expression of a constitutively active Rab5 mutant (Q79L) did not further increase the endosome size (Fig. S1 A). Rab11 exhibits some colocalization with Orai1 in oocytes but not in eggs (Fig. 1, C and D), and Rab9 distributes with Orai1-positive endosomes significantly more efficiently in eggs as compared with oocytes (Fig. 1, C and D). Similar results to Rab9 were obtained with Rab7 (Fig. S1 B). Staining with LysoTracker shows minimal colocalization with Orai1, arguing that Orai1 is not targeted to the degradative pathway (Fig. 1 C), which is consistent with Western data showing equivalent levels of Orai1 protein during meiosis (Yu et al., 2009). Collectively, these results argue that the Orai1 endocytic compartment in oocytes is the recycling endosome because Rab11 colocalizes with Orai1-positive endosomes to significantly higher levels in oocytes as compared with eggs (Fig. 1, C and D) and that the egg endosomal compartment is the late endosome because it colocalizes with both Rab9 and Rab7 in eggs to significantly higher levels than in oocytes. The localization of Orai1 to the late endosome in eggs is consistent with its dramatic internalization, as cargo from this compartment does not directly recycle back to the cell membrane (Maxfield and McGraw, 2004).

Orai1 internalization endocytic pathway

We used various approaches to define endocytic pathways through which Orai1 internalizes. Transferrin was used as a marker for clathrin-dependent endocytosis, and cholera toxin B (CTB), which binds the ganglioside GM1 (Parton, 1994), as a marker for raft-dependent endocytosis (Fig. 2 A). Orai1 colocalizes efficiently with CTB but not transferrin, arguing that Orai1 is endocytosed through a raft-dependent and clathrin-independent pathway (Fig. 2 A). CTB in different cell types can also be internalized through clathrin-dependent and caveolae- and clathrin-independent pathways (Torgersen et al., 2001; Kirkham and Parton, 2005). Therefore, the colocalization of Orai1 with CTB has to be interpreted carefully. To expand on these results, we interfered with the function of dynamin, a GTPase required for pinching endocytic vesicles during both clathrin- and Cav-dependent endocytosis (Sever, 2002). A dominant-negative dynamin mutant (K44A) abrogates Orai1 internalization, resulting in a decrease in the number and size of Orai1-positive endosomes in eggs and a steady-state enrichment of Orai1 at the cell membrane (Fig. 2 B, Dyn K44A).

Another important endocytic pathway in *Xenopus* oocytes is the Rho-dependent constitutive endocytosis (Schmalzing et al., 1995). This pathway can be inhibited using the *Clostridium botulinum* C3 exoenzyme, which ADP rybosylates RhoA, -B, and -C (Schmalzing et al., 1995). C3 exoenzyme only mildly inhibits Orai1 internalization, despite resulting in dramatic vesiculation at the cell membrane (Fig. 2 B, C3 exoenz), which is consistent with the increased membrane surface area previously described (El Jouni et al., 2007). The large vesiculations after C3 exoenzyme treatment are cell membrane invaginations, as confirmed by coexpression of TMEM16A (Fig. S1 C).

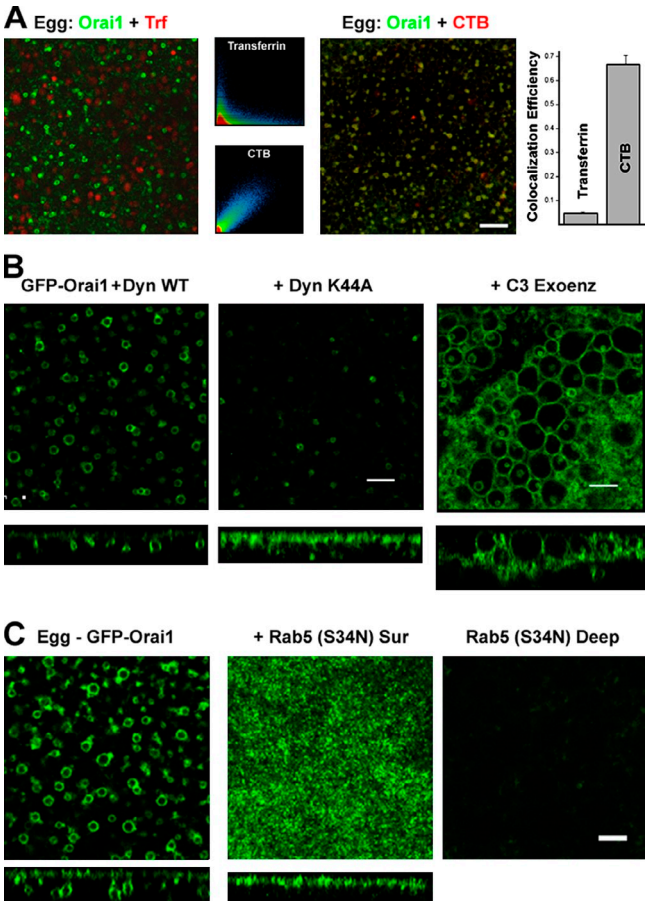

Figure 2. **Orai1 internalization endocytic pathway.** (A) Oocytes expressing GFP-Orai1 were stained with 125 µg/ml Alexa Flour 633 transferrin (Trf) or 5 µg/ml Alexa Fluor 555 CTB at the GVBD stage and allowed to complete maturation. Colocalization efficiency was measured using ZEN2008 (n = 14). Error bars indicate mean ± SEM. (B) Wild-type dynamin (WT Dyn) or the K44A mutant (30 ng/cell) were injected in GFP-Orai1–expressing cells and allowed 24 h to express before inducing maturation. C3 exoenzyme (1.7 ng/cell) was injected into GFP-Orai1–expressing cells 1 h before maturation. Images are from a focal plane ~2-µm deep from the cell surface. Orthogonal sections are also shown. (A and B) Bars, 10 µm. (C) Oocytes were injected with GFP-Orai1 alone or with 20 ng of the dominant-negative Rab5 (S34N) and then matured. Images show a deep (~2 µm into the cell) focal plane (left) or the cell surface as indicated, with the corresponding orthogonal sections. Bar, 5 µm.

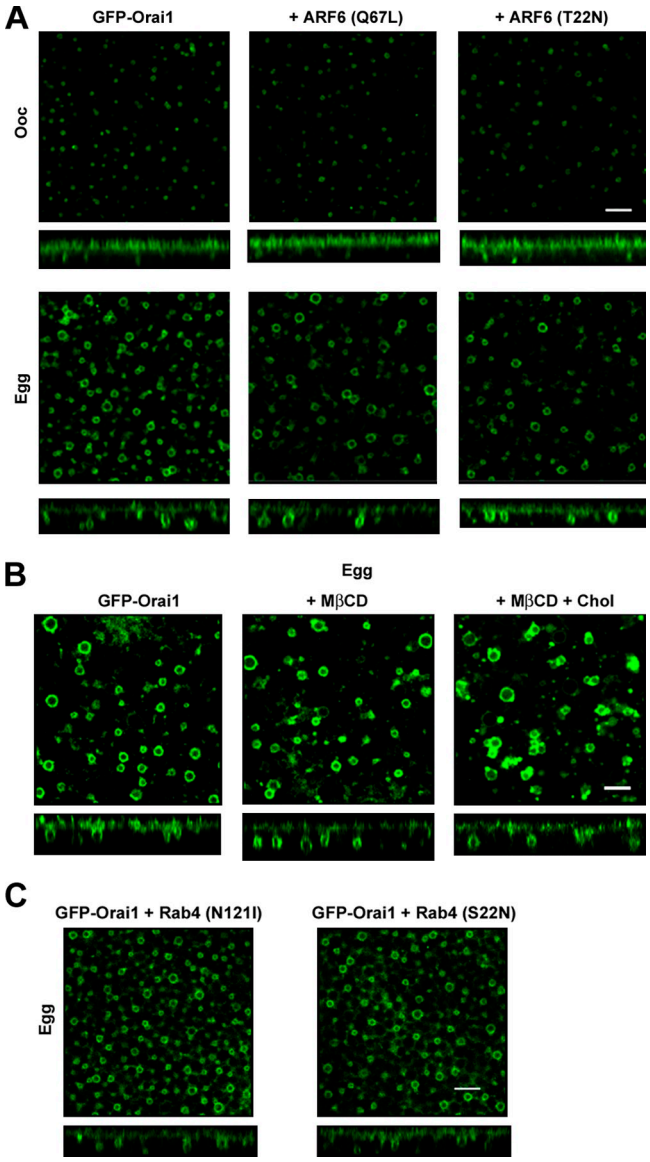

Figure 3. **Orai1 internalization: ARF6, cholesterol, and Rab4.** (A) Oocytes and eggs expressing 2 ng GFP-Orai1 alone or with 20 ng constitutively active ARF6 (Q67L) or 20 ng dominant-negative ARF6 (T22N). Orthogonal sections and deep-view images are shown. (A) GFP-Orai1–expressing oocytes were untreated, treated with 20 mM MβCD to deplete cholesterol, or treated with MβCD plus 5 mg/ml cholesterol for 9 h in Ringer, and then matured. (C) Orthogonal sections and deep-view images from eggs expressing 20 ng GFP-Orai1 and dominant-negative Rab4 mutants N121I or S22N. Bars, 5 µm.

This shows that Rho-dependent constitutive endocytosis is not the major route directing Orai1 removal from the cell membrane. This is compatible with the fact that the majority of Orai1 is removed from the cell membrane during meiosis, arguing that Orai1 is specifically targeted for endocytosis.

We also modulated ARF6-dependent endocytic pathway by injecting constitutively active (Q67L) or dominant-negative (T22N) ARF6 mutants (Fig. 3 A). Neither treatment affects Orai1 internalization during meiosis or Orai1 recycling in oocytes (Fig. 3 A), arguing that ARF6-dependent endocytosis is not involved in Orai1 trafficking.

Trafficking of Orai1 with CTB argues for potential involvement of lipid rafts, which typically entails cholesterol-rich domains that can be disrupted by methyl–β-cyclodextrin (MβCD), a cholesterol-chelating drug (Ilangumaran and Hoessli, 1998). Treating oocytes with MβCD did not affect the level of internalization of Orai1 during meiosis (Fig. 3 B). As previously reported, MβCD treatment enhanced the rate of oocyte maturation (Sadler and Jacobs, 2004), showing functionality of the drug. These data argue that Orai1 internalization does not require cholesterol. There is precedent for stable functional raft domains at the cell membrane that are cholesterol independent yet contain Cav-1 (Hansen et al., 2001).

Given the effect of Rab5 on Orai1-positive endosomes, we were interested in its potential role in mediating Orai1 internalization. A dominant-negative Rab5 mutant (S34N) effectively blocks Orai1 internalization (Fig. 2 C), revealing a requirement for Rab5 in Orai1 internalization. Rab5 has been implicated in cargo sorting and vesicle tethering and fusion (Stenmark, 2009), and, thus, its requirement for Orai1 internalization could be at

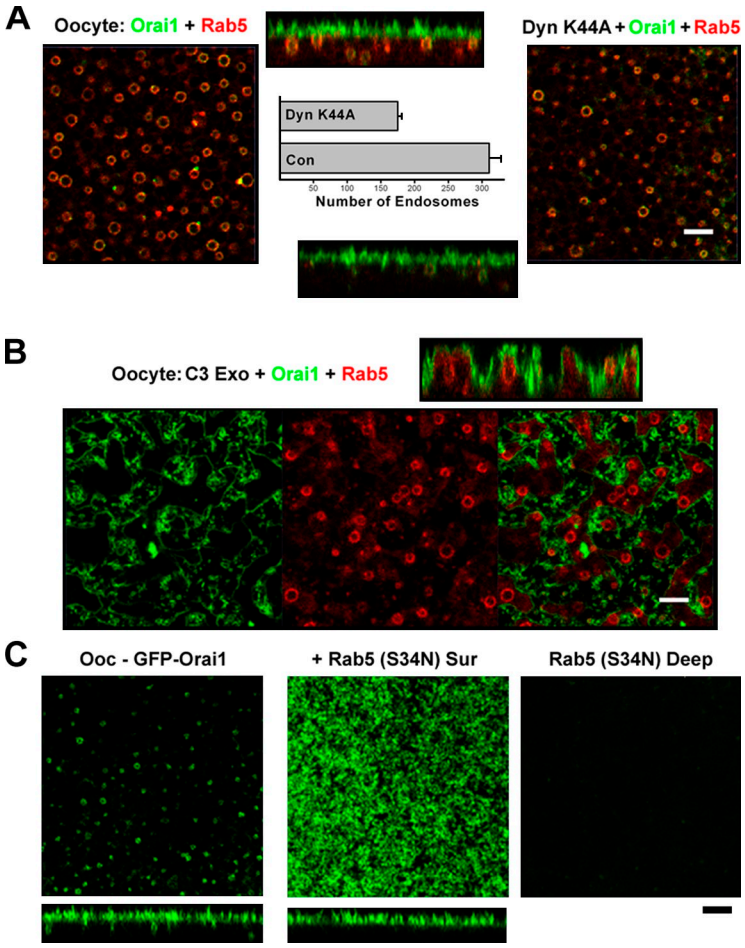

Figure 4. **Orai1-recycling endocytic pathway.** (A) Oocytes expressing 10 ng GFP-Orai1 and RFP-Rab5 were untreated or injected with dynamin (Dyn) K44A and allowed 24 h to express. Deep-view images and orthogonal sections are shown. The number of Rab5- and Orai1-positive endosomes was measured using MetaMorph (n = 9–19). Error bars indicate mean ± SEM. (B) C3 exoenzyme was injected into GFP-Orai1– and RFP-Rab5–expressing oocytes 2 h before imaging. (C) Images GFP-Orai1–injected or GFP-Orai1– and Rab5 (S34N)–coinjected oocytes. Bars, 5 µm.

multiple steps along the endocytic pathway. In contrast to Rab5, two different dominant-negative Rab4 mutants (N121I and S22N) had no effect on Orai1 internalization during meiosis (Fig. 3 C).

Orai1-recycling endocytic pathway

Using similar approaches, we dissected the endocytic pathway that underlies Orai1 recycling in oocytes. The dynamin dominant-negative mutant exhibits only a modest inhibitory effect on Orai1 recycling (Fig. 4 A) and a corresponding modest decrease in the number of recycling endosomes (Fig. S1 D). In contrast, C3 exoenzyme effectively blocks Orai1 recycling, leading to loss of Orai1 from the endocytic compartment visualized by Rab5 coexpression (Fig. 4 B). Furthermore, dominant-negative Rab5 (S34N) effectively blocks Orai1 recycling (Fig. 4 C), just as it blocked internalization during meiosis. This shows that in the interphase-like oocyte, Orai1 recycles primarily through a Rho-dependent, dynamin-independent endocytic pathway. During meiosis, Orai1 internalization switches to a dynamin-dependent, cholesterol-independent endocytic pathway.

Cav is required for Orai1 internalization but not its recycling

We have previously shown that Cav colocalizes with Orai1 in endosomes (Yu et al., 2009). To address the functional role, if any, for Cav in Orai1 internalization, we expressed either wild-type *Xenopus* Cav or a dominant-negative Cav mutant (P168L). The Cav (P168L) mutant corresponds to the P132L in human Cav (Fig. S2 A), a mutation that is frequently detected in breast cancers and seems to contribute to the generation of the metastatic phenotype (Bonuccelli et al., 2009). In contrast to the cell membrane association of wild-type Cav in both oocytes and eggs (Fig. S2 B), Cav-P168L is intracellular and localizes to both the ER and Golgi, as shown by its distribution and by coexpression of GalNAc-GFP (Fig. S2 C). The equivalent human mutation mislocalizes to the Golgi (Bonuccelli et al., 2009). Expression of Cav-P168L limits Orai1 trafficking to the cell membrane, and traps it in the ER (Fig. S2 D), thus precluding testing the role of Cav in Orai1 internalization. We circumvented this limitation by first expressing Orai1 and allowing it enrich at the cell membrane, then expressing Cav-P168L (Fig. 5 B). Under these conditions, Cav-P168L effectively inhibits Orai1 internalization, as illustrated by the reduced number of endosomes and maintenance of cell membrane enrichment of Orai1, but does not affect Orai1 recycling in the oocyte (Fig. 5 B). Overexpression of wild-type Cav with the P168L mutant rescues Orai1 internalization inhibition (Fig. 6), arguing that P168L acts by sequestering endogenous Cav. These results argue that Cav is required for Orai1 internalization during meiosis but not for its recycling in the oocyte.

Domains required for Orai1 trafficking

The complete internalization of Orai1 during meiosis argues that Orai1 is specifically targeted for endocytosis. To determine

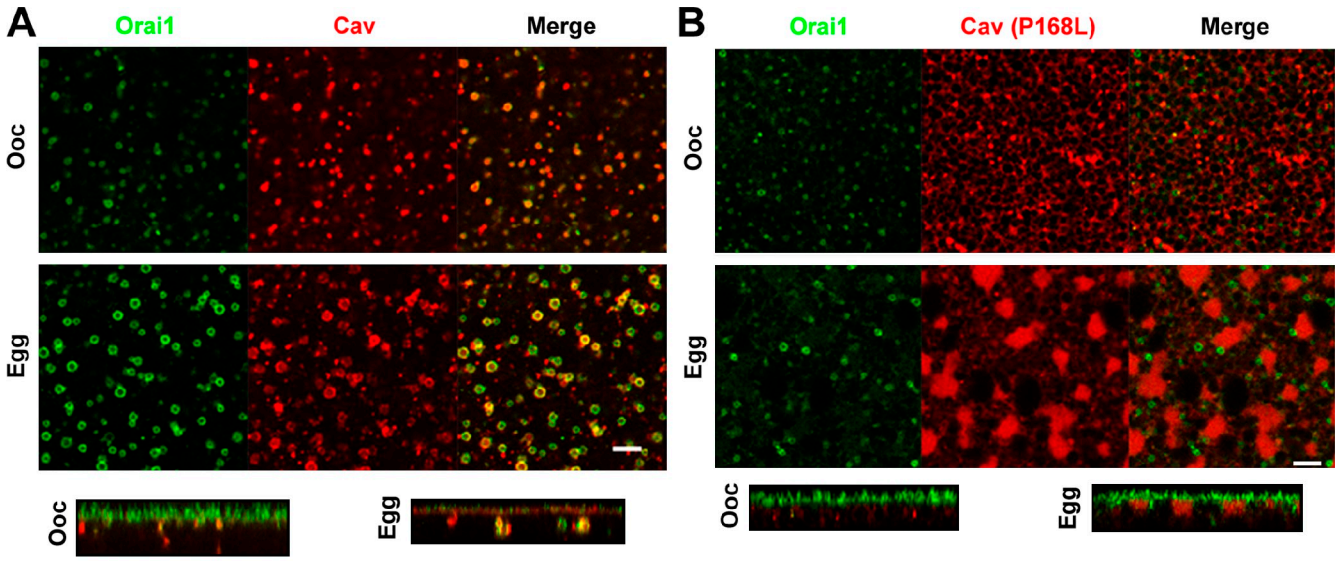

Figure 5. **Cav is required for Orai1 internalization.** (A) 10 ng GFP-Orai1– and mCherry-Cav–expressing oocytes and eggs. Images are ~2-µm deep into the cell. Orthogonal sections are also shown. (B) GFP-Orai1 was allowed to express and traffic normally for 24 h followed by expression of10 ng of the dominant-negative Cav mutant P168L 24 h before maturation. Bars, 5 µm.

which Orai1 domains are involved in this targeting, we generated different deletion mutants of Orai1 focusing primarily on the cytoplasmic N and C termini. Deletion of the entire N-terminal cytoplasmic domain (ΔN90-Orai1-CFP) decreases Orai1 trafficking to the cell membrane, trapping it primarily in the ER (Fig. 7 B and Fig. S3 A). Deleting the first 70 residues of Orai1 (ΔN70-Orai1-CFP) results in normal Orai1 trafficking to the cell membrane in oocytes; however, this mutant is not internalized during meiosis (Fig. 7 C and Fig. S3 D). This argues that sequence motifs within the first 70 residues of Orai1 are required for targeting for internalization during meiosis. Given the role of Cav in Orai1 internalization, we tested whether expression of Cav with ΔN70-Orai1 rescues its internalization defect; however, this was not the case (Fig. S3 D). In addition, ΔN70-Orai1 recycles normally in oocytes, showing that this domain is not required for Orai1 recycling.

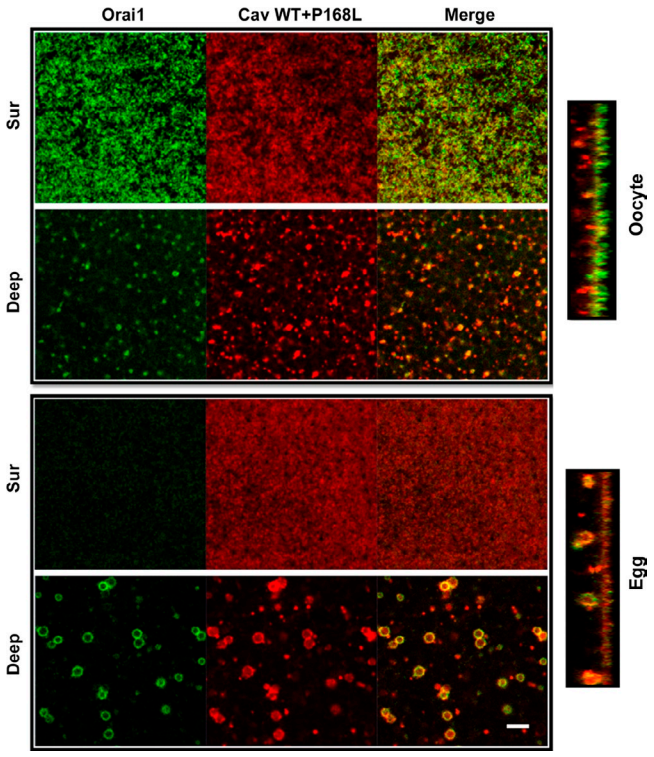

Figure 6. **Wild-type Cav rescues Orai1 internalization inhibition with Cav P168L.** Oocytes were injected with 2 ng GFP-Orai1, 10 ng Cherry-Cav (Ch-Cav) wild type (WT), and 10 ng Cherry-Cav-P168L, and then matured. Orthogonal sections and different focal plane images illustrate Orai1 and Cav distribution between the cell membrane (Sur) and endosomal compartment (Deep). Bar, 5 µm.

Deletion of the last 12 residues of Orai1 (GFP-Orai1-ΔC289) has no effect on Orai1 trafficking (Fig. 7 D and Fig. S3 C). In contrast, deletion of the entire cytoplasmic C-terminal domain (Orai1-ΔC267) inhibits Orai1 internalization without affecting trafficking to the cell membrane or recycling in oocytes (Fig. 7 E and Fig. S3 B). Interestingly, in this case, co-expression of Cav but not Rab5 effectively rescues Orai1-ΔC267 internalization (Fig. 7 E and Fig. S3 E).

The Orai1 cytoplasmic C-terminal domain is predicted to fold into a coiled-coil motif that is important for STIM1–Orai1 interaction (Zhang et al., 2006; Muik et al., 2008). To test whether Orai1 internalization requires this coiled-coil domain, we generated the L273S mutant, which is predicted to disrupt the coiled-coil and the L282S mutant, which is predicted to stabilize the coiled coil (Muik et al., 2008). Orai1-L282S traffics normally in oocytes and eggs (Fig. 7 F and Fig. S4 A), whereas the L273S mutant fails to reach the cell membrane and is retained in the ER (Fig. 7 G and Fig. S4 B). These data suggest that proper folding of the Orai1 C-terminal coiled-coil domain is important for Orai1 targeting to the cell membrane. However, because the biogenesis of Orai1-ΔC267 is unaffected, this argues that Orai1-L273S is retained in the ER because it does not fold properly.

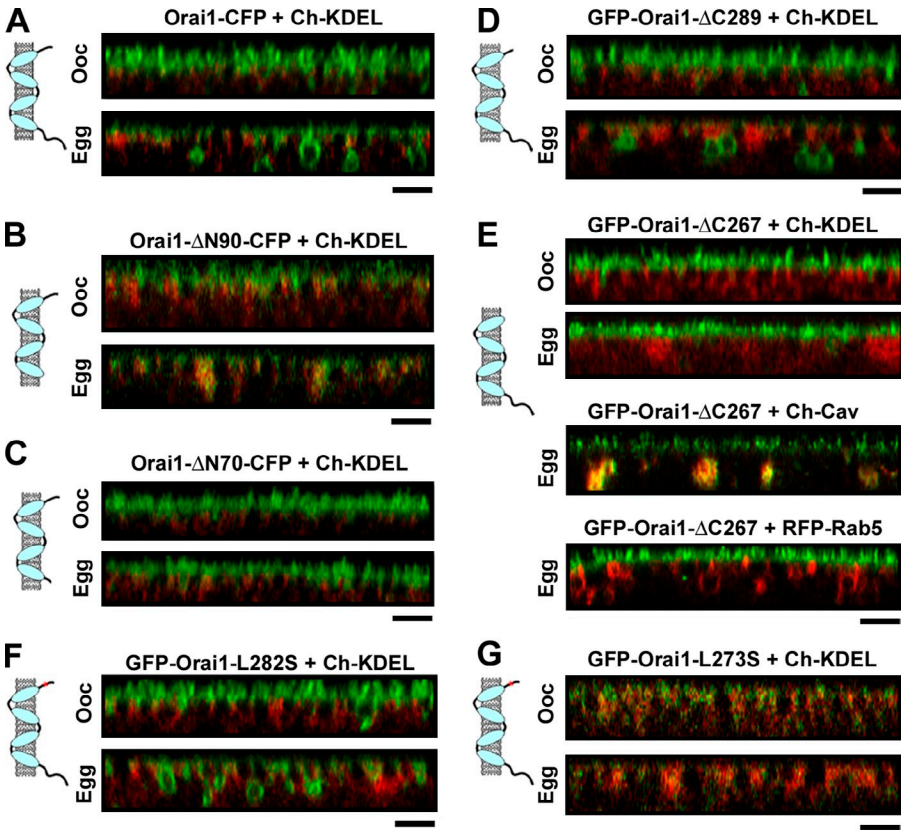

Figure 7. **Domains involved in Orai1 trafficking.** Orthogonal sections and cartoon representation for the different constructs as indicated. (A–C) Orai1 or N-terminal deletion mutants Orai1-ΔN90 and Orai1-ΔN70 tagged with CFP at the C terminus (5 ng RNA/cell) were coexpressed with Cherry-KDEL. (D) GFP-Orai1-ΔC289 (2 ng RNA/cell) is shown. (E) GFP-Orai1-ΔC267 alone or coexpressed with Cherry-Cav or RFP-Rab5. (F) GFP-Orai1-L282S traffics normally. (G) GFP-Orai1-L273S is trapped in the ER. Bars, 5 µm.

These data show that residues 267–289 in the Orai1 C-terminal cytoplasmic domain are important for effective targeting of Orai1 for endocytosis, but they are not essential because Orai1-ΔC267 can be internalized after coexpression of Cav. This argues that targeting of Orai1 for internalization depends on effective interactions between Orai1 and Cav, likely in the region within residues 1–70, because the ΔN70-Orai1 mutant is not internalized even after Cav coexpression. A Cav consensus–binding site has been identified using a peptide phage display library, as ΦXΦXXXXΦ, ΦXXXXΦXXΦ, or ΦXΦXXXXΦXXΦ (Φ indicates an aromatic amino; Couet et al., 1997). Sequence scanning of the Orai1 N terminus reveals the sequence 52-YPDWIGQSY-60, which matches an inverted Cav-binding consensus site (underlining indicates the aromatic amino acids in the sequence that match the consensus). To determine whether this region defines a Cav-binding domain, we mutated the first two aromatic residues, Y52 and W55, to Ala and tested the effect on Orai1 trafficking. Orai1-Y52,W55A traffics to the cell membrane and recycles normally in oocytes (Fig. 8 A). In contrast, during maturation, Orai1-Y52,W55A is retained at the cell membrane, showing that this Cav-binding site is required for Orai1 internalization (Fig. 8 A). If Orai1-Y52,W55A internalization block is caused by its inability to effectively interact with Cav, it is expected that coexpression of Cav will not rescue the internalization block. This is indeed the case, as shown in Fig. 8 B. Although in this case, the residual Orai1-positive endosomes are Cav positive (Fig. 8 B). In a similar fashion, coexpression of Rab5 does not affect the Orai1-Y52,W55A internalization block (Fig. 8 B). Quantification of relative cell membrane Orai1 corroborates these results (Fig. 8 C).

Orai1 contains an additional consensus Cav–binding site between residues 250 and 258 (FIVFAVHFY), which is predicted to be part of TM4 of Orai1 (Hogan et al., 2010). Because Cav inserts into the bilayer through a hairpin, this region of Orai1 could potentially interact with Cav. However, an Orai1 mutant with the first two aromatic residues mutated (F250,253A) traffics normally in oocytes and is internalized during maturation (Fig. S5 B), showing that this site is not required for Orai1 internalization.

Immunoprecipitation of wild-type Orai1 pulls down Cav, showing that Orai1 and Cav interact in vivo (Fig. 8 D). In contrast, significantly less Cav coprecipitates with Orai1-Y52,W55A, which is consistent with the inhibition of internalization of this mutant. Similar results were obtained whether Orai1 was coexpressed with human or *Xenopus* Cav (Fig. 8 D). Human Cav colocalizes with Orai1 in both oocytes and eggs (Fig. S5 A). The specificity of the anti-GFP immunoprecipitation is illustrated by the lack of Cav pull-down when the immunoprecipitation was performed using a nonspecific antigen, the inositol 1,4,5-trisphosphate receptor (Fig. 8 E).

We further generated a GFP-tagged construct that contains the first 90 residues of Orai1, either as the wild-type construct (GFP–N-term–Orai1) or with residues Y52 and W55 mutated to Ala. Both constructs express equally well, as illustrated by the Western blot (Fig. 8 F). Immunoprecipitation of wild-type GFP–N-term–Orai1 efficiently pulls down Cav, whereas the N-term–Y52,W55A mutant was significantly less effective at pulling down Cav (Fig. 8 F). The fact that some Cav coprecipitates with Orai1-Y52,W55A either in the context of the full-length protein or the N-terminal domain argues that Cav can still interact with this mutant, albeit with drastically lower efficiency. Nonetheless,

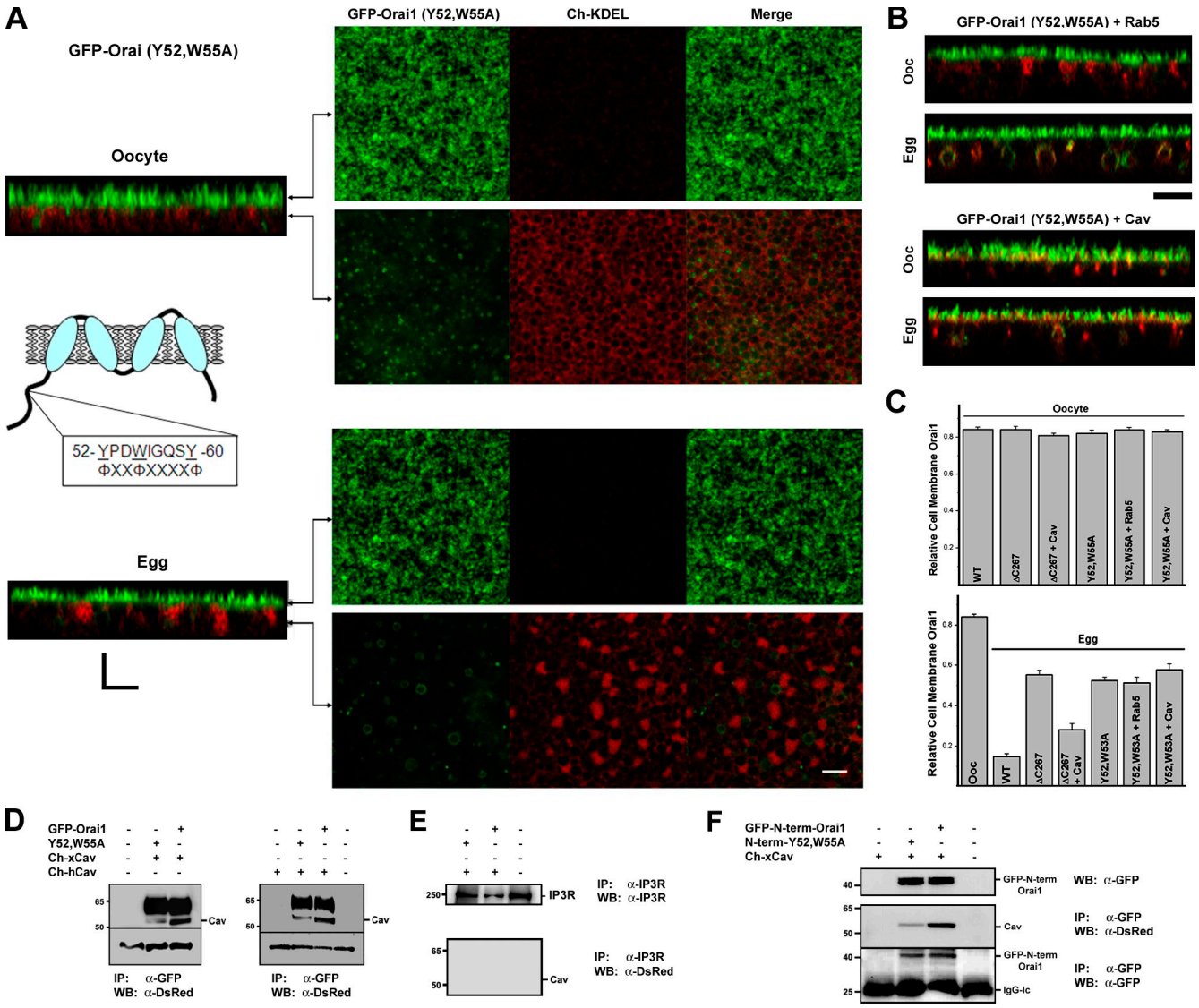

Figure 8. **Identification of a Cav-binding site in the Orai1 N terminus.** (A) The Cav consensus–binding site is illustrated in the cartoon. Cells expressing GFP-Orai1-Y52,W55A and Cherry-KDEL are shown. Planes at which the images were taken along the z stack are indicated in the orthogonal section. (B) Expression of Rab5 or Cav with Orai1-Y52,W55A does not restore its ability to internalize during meiosis. (C) Relative cell membrane Orai1 was measured as the percentage of GFP fluorescence signal on plasma membrane versus total (n = 9–38). WT, wild type. Error bars indicate mean ± SEM. (D) Orai1 was immunoprecipitated (IP) using anti-GFP antibodies from oocytes expressing 10 ng human (Ch-hCav) or *Xenopus* (Ch-xCav) Cav-1 with wild-type Orai1 or GFP-Orai1-Y52,W55A. Con indicates uninjected cells. Western blots (WB) were performed using anti-DsRed antibodies. The Cav band is indicated, also shown is a nonspecific band (~33 kD) that reacts on the Western blot as a loading control. (E) Immunoprecipitation of the IP_3 receptor (IP_3R) as a non-specific antigen does not pull down Cav, showing the specificity of the anti-GFP immunoprecipitation. (F) Oocytes were injected with GFP–N-term–Orai1, which contains residues 1–90 of Orai1. Cells were injected with wild-type GFP–N-term–Orai1 or a mutant with residues Y52 and W55 mutated to Ala (N-term–Y52,W55A). Immunoprecipitation was performed with an anti-GFP antibody and Western blots with either an anti-DsRed or anti-GFP as indicated. A Western blot of the different treatments is also shown (top). (D and F) Black lines indicate that intervening lanes have been spliced out. Bars, 5 µm.

this residual Cav association is not sufficient to mediate Orai1 internalization, even when Cav is overexpressed (Fig. 8 B).

Store depletion shifts Orai1 distribution from endosomes to the cell membrane

The fact that Orai1 recycles continuously between an endosomal compartment and the cell membrane raises the interesting question of the distribution of Orai1 after store depletion. Depleting Ca^{2+} stores in cells coexpressing STIM1 and Orai1 leads to coclustering of both proteins into large clusters referred to as puncta (Fig. 9 A). Importantly, the endosomal Orai1 pool is exhausted, arguing that recycling Orai1 is trapped by STIM1 puncta at the cell membrane, leading to depletion of the endosomal Orai1 pool. In 84% of the cells analyzed, no endosomal Orai1 was detected after store depletion (Fig. 9 A). We scored cells with any visible endosomal Orai1 as positive even if it was detected at significantly lower levels than in control cells. The presence of endosomal Orai1 after store depletion appears to correlate with lower levels of STIM1 expression.

Interestingly, rare events of intracellular STIM1–Orai1 puncta could be resolved in oocytes (Fig. 9 A, +TPEN, box). These puncta are detected deep below the membrane plane: in the example shown in Fig. 9 A, the highlighted punctum is 1.2 µm below the focal plane defined by STIM1–Orai1 puncta.

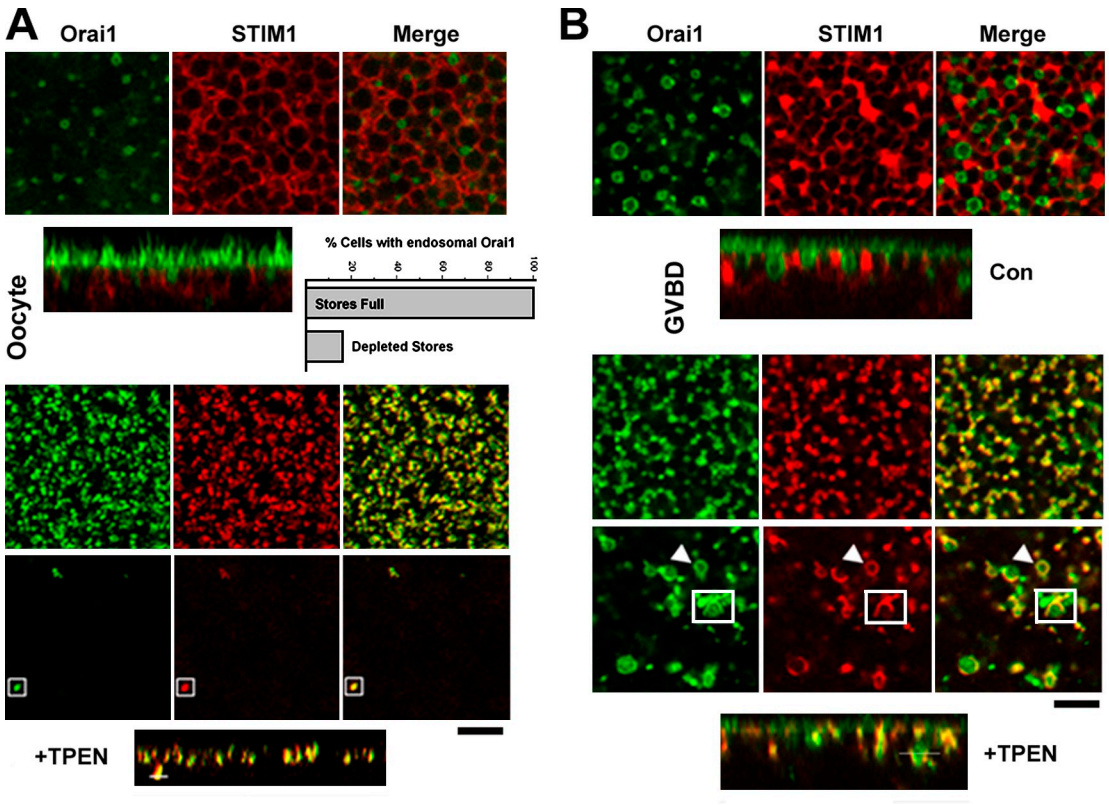

Figure 9. **Endosomal Orai1 translocates to the cell membrane after store depletion.** (A) Distribution of Orai1 and STIM1 in oocytes before and after store depletion with 5 mM TPEN, which results in coclustering of STIM1 and Orai1 at the plasma membrane–ER junction. In addition, rare coclustering events are detected deep in the cell (1.2 µm), as indicated by the boxes and matching white bar in the orthogonal section. Deep focal plane and orthogonal sections are shown. (B) Same experimental approach as in A except that images were taken at the GVBD stage of oocyte maturation. Store depletion (+TPEN) leads to Orai1–STIM1 coclustering at the cell membrane and deep in the cell at the endosome–ER interface (arrowheads and boxes). The position of the boxes is indicated by the bar in the orthogonal view. Bars, 5 µm.

This argues that as STIM1 puncta form intracellularly they can interact with intracellular Orai1 in endosomes. To further analyze this phenomenon, we imaged the behavior of STIM1 and Orai1 in response to store depletion at the germinal vesicle breakdown (GVBD) stage of meiosis. SOCE inactivates during meiosis, and this inactivation is initiated at the GVBD stage (Machaca and Haun, 2000; Yu et al., 2009). In addition, Orai1 internalization is apparent at GVBD (Fig. 9 B), thus providing a larger intracellular Orai1 pool than in the oocyte to study intracellular STIM1–Orai1 interaction. At GVBD, STIM1 and Orai1 form puncta at the cell membrane, and in addition, significant intracellular interactions are detected (Fig. 9 B, arrowhead and box). STIM1–Orai1 are detected in intracellular puncta as in the oocyte, and in addition, STIM1 coats Orai1 positive endosomes (Fig. 9 B, arrowhead). This shows that with an available intracellular Orai1 pool, clustered STIM1 can be stabilized intracellularly, which raises the potential for a functional role for these interactions in modulating Ca^{2+} dynamics after store depletion.

Discussion

Orai1 internalization

SOCE inactivates during meiosis because STIM1 does not form clusters after store depletion in the mature egg and because Orai1 is removed from the cell membrane (Yu et al., 2009). Although multiple membrane proteins are internalized during meiosis, others such as the Ca^{2+}-activated Cl^- channel, which is required for the block to polyspermy, remain enriched in the cell membrane (Fig. 1 B). This reveals specific sorting of cell membrane proteins during meiosis and argues that the subset of endocytosed proteins is specifically tagged to achieve effective internalization. This sorting is fundamental for egg activation and future embryonic development. In preparation for embryonic development, the egg internalizes both cell membrane proteins and lipids, leading to a dramatic decrease in cell membrane surface area (Kado et al., 1981; Machaca and Haun, 2000). A similar decrease in membrane surface area and modulation of vesicular trafficking has been observed during mitosis and shown to be important for M phase (Boucrot and Kirchhausen, 2007). The early rapid embryonic divisions lack the gap phases of the cell cycle required for accumulation of the molecular building blocks. Therefore, as the early blastomeres divide, they incorporate intracellularly stored vesicles rich in ionic transporters into their basolateral membrane with the apical membrane formed by the egg's cell membrane, which contains a different transporter complement (Angres et al., 1991; Gawantka et al., 1992). This results in the formation of the first polarized epithelium during embryogenesis with the capacity to transport salts and water in a vectorial fashion, and as such, contributing to the formation of the fluid-filled blastocoel cavity (Müller and

Hausen, 1995; Müller, 2001). Our experiments on the internalization of Orai1 during meiosis provide insights into the mechanisms involved in this critical development process. Orai1 is enriched at the cell membrane in oocytes and internalizes during meiosis into a late endosomal compartment that is Cav, Rab5, Rab7, and Rab9 positive. This targeted endocytosis process requires dynamin, Cav, and Rab5 and does not follow the clathrin-dependent endocytic pathway. Cav may function as a scaffolding platform to recruit the necessary molecular machinery required for Orai1 internalization, as there is evidence of a direct interaction between Cav and Rab5 (Hagiwara et al., 2009). Surprisingly, however, Orai1 internalization is independent of cholesterol, arguing that it is not through the classical lipid raft endocytic pathway. This is in contrast to the requirement for cholesterol for the internalization of the plasma membrane Ca^{2+}-ATPase during meiosis (El Jouni et al., 2008). This suggests that internalization of membrane proteins during meiosis does not follow the same endocytic pathway.

Orai1 domains involved in Orai1 internalization

We further mapped the domains within Orai1 that are required for its internalization and show that a consensus Cav–binding site in the Orai1 N terminus is essential for Orai1 endocytosis during meiosis (Fig. 8). In addition, we reveal a role for residues 267–289 in the Orai1 cytoplasmic C terminus to target Orai1 for internalization. However, this region is not essential for Orai1 internalization because Orai1-ΔC267 is internalized when coexpressed with Cav. The Orai1 C terminus is predicted to form a coiled coil required for interaction with STIM1 (Muik et al., 2008). We were not able to test whether the coiled coil by itself is required for endocytic targeting because a mutant predicted to disrupt the coiled-coil Orai1-L273S (Muik et al., 2008) did not effectively traffic to the cell membrane (Fig. 7 G). In contrast, others have shown that in mammalian cells, the L273 mutant traffics to the plasma membrane (Muik et al., 2008; Yuan et al., 2009), and in one case, the Orai1-ΔC deletion was reported to be trapped in the ER (Yuan et al., 2009). Furthermore, deletion of the N-terminal domain (Orai1-ΔN90) also disrupts Orai1 biogenesis in oocytes, although in this case, some membrane targeting is detectable (Fig. 7 B). In contrast, an Orai1 N-terminal deletion mutant has been reported to traffic normally to the plasma membrane; however, in this case, a YFP or CFP tag was placed on the N terminus (Muik et al., 2008; Park et al., 2009), whereas in our case, the CFP tag is placed on the C terminus of Orai1. This argues that the N-terminal tag may help Orai1 folding and, as such, enhance its trafficking to the cell membrane. Another study reported normal trafficking of N-terminally deleted Orai1 with a C-terminal tag (Li et al., 2007). These discrepancies in the trafficking of various Orai1 mutants may be because of different expression levels in the different studies that would drive enrichment at the cell membrane because the subcellular distribution of Orai1 is a homeostatic process that depends on the capacity of various trafficking compartments along the biogenesis and recycling pathways. Alternatively, these differences may argue for differential regulation of Orai1 trafficking in different cell types caused either by predominant active trafficking pathway and developmental stage of the cell or by accessory proteins that interact with Orai1. Indeed, the trafficking of Orai1 is quite distinct in the same cell, the *Xenopus* oocyte dependent on its developmental stage (oocyte or egg), as illustrated in this study.

Orai1 constitutive recycling

Orai1 is enriched at the cell membrane in oocytes. We estimate that ∼80% of the total Orai1 protein pool localizes to the cell membrane in *Xenopus* oocytes, this under conditions of expression of exogenous Orai1, arguing that the Orai1 trafficking machinery has a large capacity. We can also detect Orai1 recycling in CHO cells that express a YFP-tagged Orai1 (unpublished data), arguing that Orai1 recycling is conserved among different species and cell types. The constitutive recycling of Orai1 maintains a significant percentage of the total Orai1 protein pool in the recycling endosome. Importantly, store depletion results in the translocation of endosomal Orai1 to the cell membrane, where it is stabilized in STIM1–Orai1 puncta. A recent study reported an increase in surface Orai1 after store depletion (Woodard et al., 2008). However, in this case, the Orai1 increase was dependent on a rise in cytoplasmic Ca^{2+} levels, arguing that it is mechanistically different from the Orai1 translocation to the cell membrane we describe, because in our experiments, Ca^{2+} stores were depleted with TPEN, which does not involve a rise in cytoplasmic Ca^{2+} levels. Nonetheless, endosomal Orai1 represents a readily mobilizable pool of channels that could contribute to the SOCE amplitude and development kinetics. The extent of such a modulation would depend on the amount of Orai1 in the endosomal compartment relative to total cellular Orai1, on the rate of exocytosis of Orai1 from the recycling endosome, and on the levels of STIM1 relative to Orai1. Together, our experiments argue that Orai1 trafficking is an important homeostatic mechanism that regulates Orai1 levels at the cell membrane dynamically, dependent on physiological needs during cellular development.

Materials and methods

Oocyte isolation and cell culture

Xenopus laevis oocytes were prepared and handled as previously described (Machaca and Haun, 2000). TRVb-1 cells, a CHO cell line lacking the endogenous transferrin receptor and stably expressing the human transferrin receptor (McGraw et al., 1987), were grown in bicarbonate-buffered Ham's F-12 medium (Invitrogen) containing 5% FBS, 100 U/ml penicillin/streptomycin, and 200 µg/ml geneticin. Cells were grown at 37°C in a humidified atmosphere of 5% CO_2. TRVb-1 cells were transfected with HA-extra-pDS-Orai1-YFP plasmid DNA using Lipofectamine 2000 (Invitrogen) and plated onto coverslip-bottom dishes. Cells were used for experiments 48 h after transfection.

Materials

MβCD, cholesterol, and TPEN (*N*,*N*,*N*9,*N*9-Tetrakis(2-pyridylmethyl)-ethylenediamine) were obtained from Sigma-Aldrich. C3 exoenzyme was obtained from EMD. LysoTracker red DND99, Alexa Fluor 555–labeled CTB, and Alexa Fluor 633–labeled transferrin were obtained from Invitrogen.

Molecular biology

Xenopus expression plasmids pSGEM-GFP-Orai1, pSGEM-mCherry-STIM1, and pSGEM-mCherry-xCav1 were described previously (Yu et al., 2009).

Mammalian expression HA-extra-pDS-Orai1-YFP was provided by R. Lewis (Stanford University, Palo Alto, CA). xTMEM16a (GenBank/EMBL/DDBJ accession no. NM_001135237) was synthesized by imaGenes. xTMEM16a was C-terminally tagged with mCherry using PCR with primers 5′-CTTCTCAAGCTTACCATGATTATGGCCGCCAAGCTGGACG-3′ and 5′-GATATGGTACCCGGGTCACGTCCACCCGGTGGGAGTACATG-3′ and then inserted into XbaI–EcoRV pSGEM. To construct pSGEM-mCherry-KDEL, the NotI–BglII PCR fragment was subcloned into NotI–BamHI site of pSGEM with the primer pairs 5′-ACGCGGCCGCATGGTGAGCAAGGGCGA-3′ and 5′-GCTAGATCTTTAAAGTTCATCCTTTTTGTATAGTTCATCCATGC-3′. To make pSGEM-mCherry-Rab4, mCherry were amplified using primers 5′-ACGCGGCCGCATGGTGAGCAAGGGCGA-3′ and 5′-GTAGTGATATCCCGGGCTTGTACAGCTCGTCCATGCCG-3′ and was subcloned into NotI–SmaI pSGEM-Rab4. For pSGEM-mRFP-Rab5, NheI–BamHI mRFP-Rab5 (Addgene) was subcloned into XbaI–BamHI of pSGEM. Plasmids containing human Rab9, Rab11 (Addgene), and human Cav-1 (ORIGENE) were subcloned into BamHI–XhoI of pSGEM-mCherry by PCR using the following primers: Rab9, 5′-CAAGGATCCACATGGCAGGAAAATCATCAC-3′ and 5′-GTGAACTCGAGTCAACAGCAAGATGAGCTAG-3′; Rab11, 5′-CAAGGATCCACATGGGCACCCGCGACGACGAG-3′ and 5′-GTGAACTCGAGTTAGATGTTCTGACAGCACTG-3′; and human Cav, 5′-CAAGGATCCACATGTCTGGGGGCAAATACGTAGAC-3′ and 5′-GTGAACTCGAGTTATATTTCTTTCTGCAAGTTGATG-3′. To construct pSGEM-Orai1-CFP, pSGEM-Orai1-ΔN90-CFP, and pSGEM-Orai1-ΔN70-CFP, PCR fragments using the following primers were subcloned into NotI–XhoI of pSGEM: Orai1-CFP, 5′-CAGACTGCGGCCGCATGGAGCAAAAGCTCATTTCTGAG-3′ and 5′-CTGATGCTCGAGTTACTTGTACAGCTCGTCCATGCCG-3′; Orai1-ΔN90-CFP, 5′-CTTAAGCGGCCGCATGCGGACCTCGGCTCTGCTCTC-3′ and 5′-CTGATGCTCGAGTTACTTGTACAGCTCGTCCATGCCG-3′; and Orai1-ΔN70-CFP, 5′-CTTAAGCGGCCGCATGCAGGCGCTGTCCTGGCGCAAG-3′ and 5′-CTGATGCTCGAGTTACTTGTACAGCTCGTCCATGCCG-3′. To construct pSGEM-GFP-Orai1-ΔC267 and pSGEM-GFP-Orai1-ΔC289, PCR fragments using the following primers were subcloned into NotI–XhoI of pSGEM: Orai1-ΔC267, 5′-ACGCGGCCGCATGGTGAGCAAGGGCGA-3′ and 5′-GAGTGCTCGAGCTAAGTCTTATGGCTAACCAGTG-3′; and Orai1-ΔC289, 5′-ACGCGGCCGCATGGTGAGCAAGGGCGA-3′ and 5′-GAGTGCTCGAGCTAGTGGTCCAGCTGGTCCTGTAAG-3′. Plasmids containing human ARF–wild type, ARF-Q67L, and ARF-T22N (Addgene) were subcloned into BamHI–XhoI of pSGEM-mCherry by PCR using the primers 5′-CAAAGATCTCCATGGGGAAGGTGCTATC-3′ and 5′-GTGGACTCGAGTTAAGATTTGTAGTTAGAGG-3′. pSGEM-Rab4N121I and pSGEM-Rab4S22N were subcloned by inserting Rab4N121I and Rab4S22N into EcoRI site of pSGEM. GalNAc-GFP was subcloned into NotI–Klenow–EcoRI of pSGEM. To construct pSGEM-GFP-N-termOrai1 or pSGEM-GFP-N-termOrai1(Y52,W55A), the GFP–N terminus Orai1 (contains Orai1 N terminus 1–90 aa) or GFP–N terminus Orai1(Y52,W55A) fragment was subcloned into NotI–XhoI of pSGEM by PCR using primers 5′-ACGCGGCCGCATGGTGAGCAAGGGCGA-3′ and 5′-GAAGTTCTCGAGCTAGCTGGAGGCTTTAAGCTTGGCGCGGCTC-3′.

Primers for mutagenesis and tagging

xTMEM16a-mCherry (forward), 5′-CTTCTCAAGCTTACCATGATTATGGCCGCCAAGCTGGACG-3′ and (reverse) 5′-GATATGGTACCCGGGTCACGTCCACCCGGTGGGAGTACATG-3′; Rab5a S34N (forward), 5′-GTCCGCTGTTGGCAAAAACAGCCTAGTGCTTCG-3′ and (reverse) 5′-CGAAGCACTAGGCTGTTTTTGCCAACAGCGGAC-3′; Rab5a Q79L (forward), 5′-GATACAGCTGGTCTAGAACGATACCATAGC-3′ and (reverse) 5′-GCTATGGTATCGTTCTAGACCAGCTGTATC-3′; xCav-1 P168L (forward), 5′-CTGGGCAGTGGTGTTGTGCATACGAAGCTAC-3′ and (reverse) 5′-GTAGCTTCGTATGCACAACACCACTGCCCAG-3′; Orai1 L282S (forward), 5′-CTGGCGGAGTTTGCCCGCTCACAGGACCAGCTGGAC-3′ and (reverse) 5′-GTCCAGCTGGTCCTGTGAGCGGGCAAACTCCGCCAG-3′; Orai1L273S (forward), 5′-CGACAGTTCCAGGAGAGCAACGAGCTGGCGGAG-3′ and (reverse) 5′-CTCCGCCAGCTCGTTGCTCTCCTGGAACTGTCG-3′; Orai1Y52A,W55A (forward), 5′-CGTCCGCCGTCACCGCCCCGGACGCGATCGGCCAGAGTTACTC-3′ and (reverse) 5′-GAGTAACTCTGGCCGATCGCGTCCGGGGCGGTGACGGCGGACG-3′; Orai1F250A,F253A (forward), 5′-GTGCCCTTCGGCCTGATCGCTATCGTCGCCGCCGTCCACTTCTAC-3′ and (reverse) 5′-GTAGAAGTGGACGGCGGCGACGATAGCGATCAGGCCGAAGGGCAC-3′; and Orai1 T295A (forward), 5′-GACCACCCCCTGGCGCCCGGCAGCCACTATGCCTAG-3′ and (reverse) 5′-CTAGGCATAGTGGCTGCCGGGCGCCAGGGGGTGGTC-3′.

All point mutants were generated using the QuikChange mutagenesis kit (Agilent Technologies) using primers listed in Fig. S2. All mutants and constructs were verified by DNA sequencing and by analytical endonuclease restriction enzyme digestion. For in vitro transcription, after linearization with NheI, capped RNAs were transcribed in vitro using T7 RNA polymerase with T7 mMESSAGE mMACHINE kit (Applied Biosystems). Oocytes were injected with RNA and kept at 18°C in an incubator for 1–3 d after injection.

Imaging

Live cell imaging was performed on a confocal microscope (LSM710; Carl Zeiss, Inc.) using a Plan Apo 63× 1.4 NA oil differential interference contrast II objective at room temperature. Cells were normally scanned in OR2 solution (82.5 mM NaCl, 2.5 mM KCl, 1 mM $CaCl_2$, 1 mM Na_2HPO_4, and 5 mM Hepes, pH 7.5); except for experiments involving Ca^{2+} store depletion with 5 mM TPEN for 10 min at RT, cells were scanned in Ca^{2+}-free OR2 solution. Images were analyzed using ZEN 2008 (Carl Zeiss, Inc.) and MetaMorph software (MDS Analytical Technologies), and figures were compiled using Photoshop (Adobe). For the measurement of HA-Orai1-YFP exocytosis in CHO cells, images were collected on an inverted microscope (DMIRB; Leica) with a cooled charge-coupled device 12-bit camera (Princeton Instruments). All images were acquired using a 40× 1.25 NA oil objective. Cells expressing HA-Orai1-YFP were identified based on YFP fluorescence. For each time point, Cy5 and YFP images were collected by epifluorescence microscopy, and the Cy5 to YFP fluorescence of individual cells was calculated (at least 175 cells/time point/experiment). The mean Cy5 and YFP intensity per pixel was determined within each cell expressing HA-Orai1-YFP.

Immunoprecipitation

Oocytes were lysed in 30 mM Hepes, pH 7.5, 100 mM NaCl, 100 mM NaF, 2 mM sodium vanadate, 50 mM β-glycerophosphate, 10 mM sodium pyrophosphate, 5 mM EDTA, 5 mM EGTA, 1 mM DTT, and protease inhibitor cocktail III. Crude lysates were centrifuged three times at 1,000 *g* at 4°C for 10 min to remove yolk platelets. NP-40 was then added to a final concentration of 4% followed by incubation at 4°C for 2 h with constant shaking. Lysates were centrifuged at 20,000 *g* for 20 min. Orai1 was immunoprecipitated using an anti-GFP full-length polyclonal antibody (Takara Bio Inc.) and protein A/G plus agarose beads (Santa Cruz Biotechnology, Inc.). Western blotting was performed using an anti-DsRed monoclonal antibody (Takara Bio Inc.).

Online supplemental material

Fig. S1 shows further characterization of Rabs and dynamin on Orai1 trafficking. Fig. S2 shows the subcellular distribution of the Cav dominant-negative mutant P168L. Fig. S3 shows further characterization of the trafficking of different Orai1 deletions. Fig. S4 shows the subcellular distribution of Orai1 C terminus point mutants. Fig. S5 shows colocalization of GFP-Orai1 with human Cav. Online supplemental material is available at http://www.jcb.org/cgi/content/full/jcb.201006022/DC1.

We are grateful to the following laboratories for sharing clones: Rich Lewis for HA-extra-pDS-Orai1-YFP, Peter Van der Sluijs for pcDNA3-Rab4N121I and pcDNA3-Rab4S22N, Brian Storrie for GalNAc-GFP, and Mark Terasaki for GFP-KDEL. We thank Shirley Haun for subcloning several of the initial constructs, Satanay Hubrack for help with the co-immunoprecipitation experiments, and the Weill Cornell Medical College in Qatar genomics core for sequencing various mutants.

This work was funded by grants from the Qatar National Research Fund (NPRP08-395-3-088 and NPRP08-138-3-050) and the National Institutes of Health (GM61829). The statements made herein are solely the responsibility of the authors.

Submitted: 3 June 2010
Accepted: 4 October 2010

References

Alderton, J.M., S.A. Ahmed, L.A. Smith, and R.A. Steinhardt. 2000. Evidence for a vesicle-mediated maintenance of store-operated calcium channels in a human embryonic kidney cell line. *Cell Calcium.* 28:161–169. doi:10.1054/ceca.2000.0144

Angres, B., A.H. Müller, J. Kellermann, and P. Hausen. 1991. Differential expression of two cadherins in *Xenopus laevis*. *Development.* 111:829–844.

Bakowski, D., R.D. Burgoyne, and A.B. Parekh. 2003. Activation of the store-operated calcium current ICRAC can be dissociated from regulated exocytosis in rat basophilic leukaemia (RBL-1) cells. *J. Physiol.* 553:387–393. doi:10.1113/jphysiol.2003.055335

Bezzerides, V.J., I.S. Ramsey, S. Kotecha, A. Greka, and D.E. Clapham. 2004. Rapid vesicular translocation and insertion of TRP channels. *Nat. Cell Biol.* 6:709–720. doi:10.1038/ncb1150

Bonuccelli, G., M.C. Casimiro, F. Sotgia, C. Wang, M. Liu, S. Katiyar, J. Zhou, E. Dew, F. Capozza, K.M. Daumer, et al. 2009. Caveolin-1 (P132L), a common breast cancer mutation, confers mammary cell invasiveness and defines a novel stem cell/metastasis-associated gene signature. *Am. J. Pathol.* 174:1650–1662. doi:10.2353/ajpath.2009.080648

Boucrot, E., and T. Kirchhausen. 2007. Endosomal recycling controls plasma membrane area during mitosis. *Proc. Natl. Acad. Sci. USA.* 104:7939–7944. doi:10.1073/pnas.0702511104

Brazer, S.C., B.B. Singh, X. Liu, W. Swaim, and I.S. Ambudkar. 2003. Caveolin-1 contributes to assembly of store-operated Ca2+ influx channels by regulating plasma membrane localization of TRPC1. *J. Biol. Chem.* 278:27208–27215. doi:10.1074/jbc.M301118200

Couet, J., S. Li, T. Okamoto, T. Ikezu, and M.P. Lisanti. 1997. Identification of peptide and protein ligands for the caveolin-scaffolding domain. Implications for the interaction of caveolin with caveolae-associated proteins. *J. Biol. Chem.* 272:6525–6533. doi:10.1074/jbc.272.48.30429

El-Jouni, W., S. Haun, R. Hodeify, A. Hosein Walker, and K. Machaca. 2007. Vesicular traffic at the cell membrane regulates oocyte meiotic arrest. *Development.* 134:3307–3315. doi:10.1242/dev.005454

El-Jouni, W., S. Haun, and K. Machaca. 2008. Internalization of plasma membrane Ca2+-ATPase during *Xenopus* oocyte maturation. *Dev. Biol.* 324:99–107. doi:10.1016/j.ydbio.2008.09.007

Fahrner, M., M. Muik, I. Derler, R. Schindl, R. Fritsch, I. Frischauf, and C. Romanin. 2009. Mechanistic view on domains mediating STIM1-Orai coupling. *Immunol. Rev.* 231:99–112. doi:10.1111/j.1600-065X.2009.00815.x

Fasolato, C., M. Hoth, and R. Penner. 1993. A GTP-dependent step in the activation mechanism of capacitative calcium influx. *J. Biol. Chem.* 268:20737–20740.

Feske, S., Y. Gwack, M. Prakriya, S. Srikanth, S.H. Puppel, B. Tanasa, P.G. Hogan, R.S. Lewis, M. Daly, and A. Rao. 2006. A mutation in Orai1 causes immune deficiency by abrogating CRAC channel function. *Nature.* 441:179–185. doi:10.1038/nature04702

Gawantka, V., H. Ellinger-Ziegelbauer, and P. Hausen. 1992. Beta 1-integrin is a maternal protein that is inserted into all newly formed plasma membranes during early *Xenopus* embryogenesis. *Development.* 115:595–605.

Gregory, R.B., and G.J. Barritt. 1996. Store-activated Ca^{2+} inflow in *Xenopus laevis* oocytes: inhibition by primaquine and evaluation of the role of membrane fusion. *Biochem. J.* 319:755–760.

Hagiwara, M., Y. Shirai, R. Nomura, M. Sasaki, K. Kobayashi, T. Tadokoro, and Y. Yamamoto. 2009. Caveolin-1 activates Rab5 and enhances endocytosis through direct interaction. *Biochem. Biophys. Res. Commun.* 378:73–78. doi:10.1016/j.bbrc.2008.10.172

Hansen, G.H., L. Immerdal, E. Thorsen, L.L. Niels-Christiansen, B.T. Nystrøm, E.J. Demant, and E.M. Danielsen. 2001. Lipid rafts exist as stable cholesterol-independent microdomains in the brush border membrane of enterocytes. *J. Biol. Chem.* 276:32338–32344. doi:10.1074/jbc.M102667200

Hogan, P.G., R.S. Lewis, and A. Rao. 2010. Molecular basis of calcium signaling in lymphocytes: STIM and ORAI. *Annu. Rev. Immunol.* 28:491–533. doi:10.1146/annurev.immunol.021908.132550

Huang, G.N., W. Zeng, J.Y. Kim, J.P. Yuan, L. Han, S. Muallem, and P.F. Worley. 2006. STIM1 carboxyl-terminus activates native SOC, I(crac) and TRPC1 channels. *Nat. Cell Biol.* 8:1003–1010. doi:10.1038/ncb1454

Ilangumaran, S., and D.C. Hoessli. 1998. Effects of cholesterol depletion by cyclodextrin on the sphingolipid microdomains of the plasma membrane. *Biochem. J.* 335:433–440.

Kado, R.T., K. Marcher, and R. Ozon. 1981. Electrical membrane properties of the *Xenopus laevis* oocyte during progesterone-induced meiotic maturation. *Dev. Biol.* 84:471–476. doi:10.1016/0012-1606(81)90417-6

Kirkham, M., and R.G. Parton. 2005. Clathrin-independent endocytosis: new insights into caveolae and non-caveolar lipid raft carriers. *Biochim. Biophys. Acta.* 1746:349–363. doi:10.1016/j.bbamcr.2005.11.007

Lee, K.P., J.P. Yuan, J.H. Hong, I. So, P.F. Worley, and S. Muallem. 2010. An endoplasmic reticulum/plasma membrane junction: STIM1/Orai1/TRPCs. *FEBS Lett.* 584:2022–2027. doi:10.1016/j.febslet.2009.11.078

Lewis, R.S. 2007. The molecular choreography of a store-operated calcium channel. *Nature.* 446:284–287. doi:10.1038/nature05637

Li, Z., J. Lu, P. Xu, X. Xie, L. Chen, and T. Xu. 2007. Mapping the interacting domains of STIM1 and Orai1 in Ca2+ release-activated Ca2+ channel activation. *J. Biol. Chem.* 282:29448–29456. doi:10.1074/jbc.M703573200

Liou, J., M.L. Kim, W.D. Heo, J.T. Jones, J.W. Myers, J.E. Ferrell Jr., and T. Meyer. 2005. STIM is a Ca2+ sensor essential for Ca2+-store-depletion-triggered Ca2+ influx. *Curr. Biol.* 15:1235–1241. doi:10.1016/j.cub.2005.05.055

Liou, J., M. Fivaz, T. Inoue, and T. Meyer. 2007. Live-cell imaging reveals sequential oligomerization and local plasma membrane targeting of stromal interaction molecule 1 after Ca2+ store depletion. *Proc. Natl. Acad. Sci. USA.* 104:9301–9306. doi:10.1073/pnas.0702866104

Lockwich, T.P., X. Liu, B.B. Singh, J. Jadlowiec, S. Weiland, and I.S. Ambudkar. 2000. Assembly of Trp1 in a signaling complex associated with caveolin-scaffolding lipid raft domains. *J. Biol. Chem.* 275:11934–11942. doi:10.1074/jbc.275.16.11934

Luik, R.M., M.M. Wu, J. Buchanan, and R.S. Lewis. 2006. The elementary unit of store-operated Ca^{2+} entry: local activation of CRAC channels by STIM1 at ER–plasma membrane junctions. *J. Cell Biol.* 174:815–825. doi:10.1083/jcb.200604015

Machaca, K. 2007. Ca2+ signaling differentiation during oocyte maturation. *J. Cell. Physiol.* 213:331–340. doi:10.1002/jcp.21194

Machaca, K., and S. Haun. 2000. Store-operated calcium entry inactivates at the germinal vesicle breakdown stage of *Xenopus* meiosis. *J. Biol. Chem.* 275:38710–38715. doi:10.1074/jbc.M007887200

Machaca, K., and S. Haun. 2002. Induction of maturation-promoting factor during *Xenopus* oocyte maturation uncouples Ca^{2+} store depletion from store-operated Ca^{2+} entry. *J. Cell Biol.* 156:75–85. doi:10.1083/jcb.200110059

Machaca, K., Z. Qu, A. Kuruma, H.C. Hartzell, and N. McCarty. 2001. The endogenous calcium-activated Cl channel in *Xenopus* oocytes: a physiologically and biophysically rich model system. *In* Calcium Activates Chloride Channels. C.M. Fuller, editor. Academic Press, San Diego. 3–39.

Masui, Y., and H.J. Clarke. 1979. Oocyte maturation. *Int. Rev. Cytol.* 57:185–282. doi:10.1016/S0074-7696(08)61464-3

Maxfield, F.R., and T.E. McGraw. 2004. Endocytic recycling. *Nat. Rev. Mol. Cell Biol.* 5:121–132. doi:10.1038/nrm1315

McGraw, T.E., L. Greenfield, and F.R. Maxfield. 1987. Functional expression of the human transferrin receptor cDNA in Chinese hamster ovary cells deficient in endogenous transferrin receptor. *J. Cell Biol.* 105:207–214. doi:10.1083/jcb.105.1.207

Muik, M., I. Frischauf, I. Derler, M. Fahrner, J. Bergsmann, P. Eder, R. Schindl, C. Hesch, B. Polzinger, R. Fritsch, et al. 2008. Dynamic coupling of the putative coiled-coil domain of ORAI1 with STIM1 mediates ORAI1 channel activation. *J. Biol. Chem.* 283:8014–8022. doi:10.1074/jbc.M708898200

Müller, H.A. 2001. Of mice, frogs and flies: generation of membrane asymmetries in early development. *Dev. Growth Differ.* 43:327–342. doi:10.1046/j.1440-169x.2001.00587.x

Müller, H.A., and P. Hausen. 1995. Epithelial cell polarity in early *Xenopus* development. *Dev. Dyn.* 202:405–420.

Orci, L., M. Ravazzola, M. Le Coadic, W.W. Shen, N. Demaurex, and P. Cosson. 2009. From the cover: STIM1-induced precortical and cortical subdomains of the endoplasmic reticulum. *Proc. Natl. Acad. Sci. USA.* 106:19358–19362. doi:10.1073/pnas.0911280106

Pani, B., H.L. Ong, S.C. Brazer, X. Liu, K. Rauser, B.B. Singh, and I.S. Ambudkar. 2009. Activation of TRPC1 by STIM1 in ER-PM microdomains involves release of the channel from its scaffold caveolin-1. *Proc. Natl. Acad. Sci. USA.* 106:20087–20092.

Park, C.Y., P.J. Hoover, F.M. Mullins, P. Bachhawat, E.D. Covington, S. Raunser, T. Walz, K.C. Garcia, R.E. Dolmetsch, and R.S. Lewis. 2009. STIM1 clusters and activates CRAC channels via direct binding of a cytosolic domain to Orai1. *Cell.* 136:876–890. doi:10.1016/j.cell.2009.02.014

Parton, R.G. 1994. Ultrastructural localization of gangliosides; GM1 is concentrated in caveolae. *J. Histochem. Cytochem.* 42:155–166.

Patterson, R.L., D.B. van Rossum, and D.L. Gill. 1999. Store-operated Ca2+ entry: evidence for a secretion-like coupling model. *Cell.* 98:487–499. doi:10.1016/S0092-8674(00)81977-7

Perrin, M.J., R.N. Subbiah, J.I. Vandenberg, and A.P. Hill. 2008. Human ether-a-go-go related gene (hERG) K+ channels: function and dysfunction. *Prog. Biophys. Mol. Biol.* 98:137–148. doi:10.1016/j.pbiomolbio.2008.10.006

Prakriya, M., S. Feske, Y. Gwack, S. Srikanth, A. Rao, and P.G. Hogan. 2006. Orai1 is an essential pore subunit of the CRAC channel. *Nature.* 443:230–233. doi:10.1038/nature05122

Preston, S.F., R.I. Sha'afi, and R.D. Berlin. 1991. Regulation of Ca^{2+} influx during mitosis: Ca^{2+} influx and depletion of intracellular Ca^{2+} stores are coupled in interphase but not mitosis. *Cell Regul.* 2:915–925.

Roos, J., P.J. DiGregorio, A.V. Yeromin, K. Ohlsen, M. Lioudyno, S. Zhang, O. Safrina, J.A. Kozak, S.L. Wagner, M.D. Cahalan, et al. 2005. STIM1, an essential and conserved component of store-operated Ca^{2+} channel function. *J. Cell Biol.* 169:435–445. doi:10.1083/jcb.200502019

Rosado, J.A., S. Jenner, and S.O. Sage. 2000. A role for the actin cytoskeleton in the initation and maintenance of store-mediated calcium entry in human platelets. *J. Biol. Chem.* 275:7527–7533. doi:10.1074/jbc.275.11.7527

Sadler, S.E., and N.D. Jacobs. 2004. Stimulation of *Xenopus laevis* oocyte maturation by methyl-beta-cyclodextrin. *Biol. Reprod.* 70:1685–1692. doi:10.1095/biolreprod.103.026161

Schmalzing, G., H.P. Richter, A. Hansen, W. Schwarz, I. Just, and K. Aktories. 1995. Involvement of the GTP binding protein Rho in constitutive endocytosis in *Xenopus laevis* oocytes. *J. Cell Biol.* 130:1319–1332. doi:10.1083/jcb.130.6.1319

Schroeder, B.C., T. Cheng, Y.N. Jan, and L.Y. Jan. 2008. Expression cloning of TMEM16A as a calcium-activated chloride channel subunit. *Cell.* 134:1019–1029. doi:10.1016/j.cell.2008.09.003

Scott, C.C., W. Furuya, W.S. Trimble, and S. Grinstein. 2003. Activation of store-operated calcium channels: assessment of the role of snare-mediated vesicular transport. *J. Biol. Chem.* 278:30534–30539. doi:10.1074/jbc.M304718200

Sever, S. 2002. Dynamin and endocytosis. *Curr. Opin. Cell Biol.* 14:463–467. doi:10.1016/S0955-0674(02)00347-2

Singh, B.B., T.P. Lockwich, B.C. Bandyopadhyay, X. Liu, S. Bollimuntha, S.C. Brazer, C. Combs, S. Das, A.G. Leenders, Z.H. Sheng, et al. 2004. VAMP2-dependent exocytosis regulates plasma membrane insertion of TRPC3 channels and contributes to agonist-stimulated Ca2+ influx. *Mol. Cell.* 15:635–646. doi:10.1016/j.molcel.2004.07.010

Skach, W.R. 2000. Defects in processing and trafficking of the cystic fibrosis transmembrane conductance regulator. *Kidney Int.* 57:825–831. doi:10.1046/j.1523-1755.2000.00921.x

Somasundaram, B., J.C. Norman, and M.P. Mahaut-Smith. 1995. Primaquine, an inhibitor of vesicular transport, blocks the calcium-release-activated current in rat megakaryocytes. *Biochem. J.* 309:725–729.

Stathopulos, P.B., L. Zheng, G.Y. Li, M.J. Plevin, and M. Ikura. 2008. Structural and mechanistic insights into STIM1-mediated initiation of store-operated calcium entry. *Cell.* 135:110–122. doi:10.1016/j.cell.2008.08.006

Stenmark, H. 2009. Rab GTPases as coordinators of vesicle traffic. *Nat. Rev. Mol. Cell Biol.* 10:513–525. doi:10.1038/nrm2728

Tani, D., M.K. Monteilh-Zoller, A. Fleig, and R. Penner. 2007. Cell cycle-dependent regulation of store-operated I(CRAC) and Mg2+-nucleotide-regulated MagNuM (TRPM7) currents. *Cell Calcium.* 41:249–260. doi:10.1016/j.ceca.2006.07.004

Torgersen, M.L., G. Skretting, B. van Deurs, and K. Sandvig. 2001. Internalization of cholera toxin by different endocytic mechanisms. *J. Cell Sci.* 114:3737–3747.

Ullah, G., P. Jung, and K. Machaca. 2007. Modeling Ca2+ signaling differentiation during oocyte maturation. *Cell Calcium.* 42:556–564. doi:10.1016/j.ceca.2007.01.010

Vig, M., C. Peinelt, A. Beck, D.L. Koomoa, D. Rabah, M. Koblan-Huberson, S. Kraft, H. Turner, A. Fleig, R. Penner, and J.P. Kinet. 2006. CRACM1 is a plasma membrane protein essential for store-operated Ca2+ entry. *Science.* 312:1220–1223. doi:10.1126/science.1127883

Woodard, G.E., G.M. Salido, and J.A. Rosado. 2008. Enhanced exocytotic-like insertion of Orai1 into the plasma membrane upon intracellular Ca2+ store depletion. *Am. J. Physiol. Cell Physiol.* 294:C1323–C1331. doi:10.1152/ajpcell.00071.2008

Wu, M.M., J. Buchanan, R.M. Luik, and R.S. Lewis. 2006. Ca^{2+} store depletion causes STIM1 to accumulate in ER regions closely associated with the plasma membrane. *J. Cell Biol.* 174:803–813. doi:10.1083/jcb.200604014

Yang, Y.D., H. Cho, J.Y. Koo, M.H. Tak, Y. Cho, W.S. Shim, S.P. Park, J. Lee, B. Lee, B.M. Kim, et al. 2008. TMEM16A confers receptor-activated calcium-dependent chloride conductance. *Nature.* 455:1210–1215. doi:10.1038/nature07313

Yao, Y., A.V. Ferrer-Montiel, M. Montal, and R.Y. Tsien. 1999. Activation of store-operated Ca2+ current in *Xenopus* oocytes requires SNAP-25 but not a diffusible messenger. *Cell.* 98:475–485. doi:10.1016/S0092-8674(00)81976-5

Yeromin, A.V., S.L. Zhang, W. Jiang, Y. Yu, O. Safrina, and M.D. Cahalan. 2006. Molecular identification of the CRAC channel by altered ion selectivity in a mutant of Orai. *Nature.* 443:226–229. doi:10.1038/nature05108

Yu, F., L. Sun, and K. Machaca. 2009. Orai1 internalization and STIM1 clustering inhibition modulate SOCE inactivation during meiosis. *Proc. Natl. Acad. Sci. USA.* 106:17401–17406. doi:10.1073/pnas.0904651106

Yuan, J.P., W. Zeng, G.N. Huang, P.F. Worley, and S. Muallem. 2007. STIM1 heteromultimerizes TRPC channels to determine their function as store-operated channels. *Nat. Cell Biol.* 9:636–645. doi:10.1038/ncb1590

Yuan, J.P., W. Zeng, M.R. Dorwart, Y.J. Choi, P.F. Worley, and S. Muallem. 2009. SOAR and the polybasic STIM1 domains gate and regulate Orai channels. *Nat. Cell Biol.* 11:337–343. doi:10.1038/ncb1842

Zhang, S.L., A.V. Yeromin, X.H. Zhang, Y. Yu, O. Safrina, A. Penna, J. Roos, K.A. Stauderman, and M.D. Cahalan. 2006. Genome-wide RNAi screen of Ca(2+) influx identifies genes that regulate Ca(2+) release-activated Ca(2+) channel activity. *Proc. Natl. Acad. Sci. USA.* 103:9357–9362. doi:10.1073/pnas.0603161103